

The following resources related to this article are available online at www.sciencemag.org (this information is current as of November 11, 2009):

Updated information and services, including high-resolution figures, can be found in the online version of this article at:

<http://www.sciencemag.org/cgi/content/full/317/5841/1087>

Supporting Online Material can be found at:

<http://www.sciencemag.org/cgi/content/full/317/5841/1087/DC1>

This article **cites 17 articles**, 6 of which can be accessed for free:

<http://www.sciencemag.org/cgi/content/full/317/5841/1087#otherarticles>

This article has been **cited by** 8 article(s) on the ISI Web of Science.

This article has been **cited by** 10 articles hosted by HighWire Press; see:

<http://www.sciencemag.org/cgi/content/full/317/5841/1087#otherarticles>

This article appears in the following **subject collections**:

Molecular Biology

http://www.sciencemag.org/cgi/collection/molec_biol

Information about obtaining **reprints** of this article or about obtaining **permission to reproduce this article** in whole or in part can be found at:

<http://www.sciencemag.org/about/permissions.dtl>

CHD1 Motor Protein Is Required for Deposition of Histone Variant H3.3 into Chromatin in Vivo

Alexander Y. Konev,¹ Martin Tribus,² Sung Yeon Park,³ Valerie Podhraski,² Chin Yan Lim,^{4*} Alexander V. Emelyanov,¹ Elena Vershilova,¹ Vincenzo Pirrotta,³ James T. Kadonaga,⁴ Alexandra Lusser,^{2†} Dmitry V. Fyodorov^{1†}

The organization of chromatin affects all aspects of nuclear DNA metabolism in eukaryotes. H3.3 is an evolutionarily conserved histone variant and a key substrate for replication-independent chromatin assembly. Elimination of chromatin remodeling factor CHD1 in *Drosophila* embryos abolishes incorporation of H3.3 into the male pronucleus, renders the paternal genome unable to participate in zygotic mitoses, and leads to the development of haploid embryos. Furthermore, CHD1, but not ISWI, interacts with HIRA in cytoplasmic extracts. Our findings establish CHD1 as a major factor in replacement histone metabolism in the nucleus and reveal a critical role for CHD1 in the earliest developmental instances of genome-scale, replication-independent nucleosome assembly. Furthermore, our results point to the general requirement of adenosine triphosphate (ATP)-utilizing motor proteins for histone deposition in vivo.

Histone-DNA interactions constantly change during various processes of DNA metabolism. Recent studies have highlighted the importance of histone variants, such as H3.3, CENP-A (centromere protein A), or H2A.Z, in chromatin dynamics (1, 2). Incorporation of replacement histones into chromatin occurs throughout the cell cycle, whereas nucleosomes containing canonical histones are assembled exclusively during DNA replication. A thorough understanding of the replication-independent mechanisms of chromatin assembly, however, is lacking.

In vitro, chromatin assembly requires the action of histone chaperones and adenosine triphosphate (ATP)-utilizing factors (3). Histone chaperones may specialize for certain histone variants. For example, H3.3 associates with a complex containing HIRA, whereas canonical H3 is in a complex with CAF-1 (chromatin assembly factor 1) (4). The molecular motors known to assemble nucleosomes are ACF (ATP-utilizing chromatin assembly and remodeling factor), CHRAC (chromatin accessibility complex), and RSF (nucleosome-remodeling and spacing factor), which contain the Snf2 family member ISWI as the catalytic subunit (5–7), and CHD1, which belongs to the CHD subfamily of Snf2-like adenosine triphosphatases (ATPases) (8). These factors have not been shown to mediate

deposition of histones in vivo. We previously demonstrated that CHD1, together with the chaperone NAP-1, assembles nucleosome arrays from DNA and histones in vitro (9). Here, we investigated the role of CHD1 in chromatin assembly in vivo in *Drosophila*.

We generated *Chd1* alleles by P element-mediated mutagenesis (Fig. 1A) (10). Two exci-

sions, *Df(2L)Chd1[1]* and *Df(2L)Chd1[2]*, deleted fragments of the *Chd1* gene and fragments of unrelated adjacent genes. Heterozygous combinations, however, of *Chd1[1]* or *Chd1[2]* with *Df(2L)Exel7014* affect both copies of the *Chd1* gene only (Fig. 1B). We also identified a single point mutation that results in premature translation termination of *Chd1* (Q1394*) in a previously described lethal allele, *l(2)23Cd[A7-4]* (11). Hence, *l(2)23Cd[A7-4]* was renamed *Chd1[3]*.

Analysis of Western blots of embryos from heterozygous *Chd1[3]* fruit flies revealed the presence of a truncated polypeptide besides full-length CHD1 (Fig. 1C). No truncated polypeptides were detected in heterozygous *Chd1[1]* or *Chd1[2]* embryos. Therefore, the corresponding deficiencies result in null mutations of *Chd1*. Crosses of heterozygous *Chd1* mutant alleles with *Df(2L)JS17/CyO* or *Df(2L)Exel7014/CyO* produced subviable adult homozygous mutant progeny (fig. S1). Both males and females were sterile. Homozygous null females mated to wild-type males laid fertilized eggs that died before hatching. Therefore, maternal CHD1 is essential for embryonic development.

When we examined the chromosome structure of 0- to 4-hour-old embryos laid by *Chd1*-null females, we observed that, during syncytial mitoses (cycles 3 to 13), the nuclei appeared to be abnormally small. The observed numbers of anaphase chromosomes suggested that they were

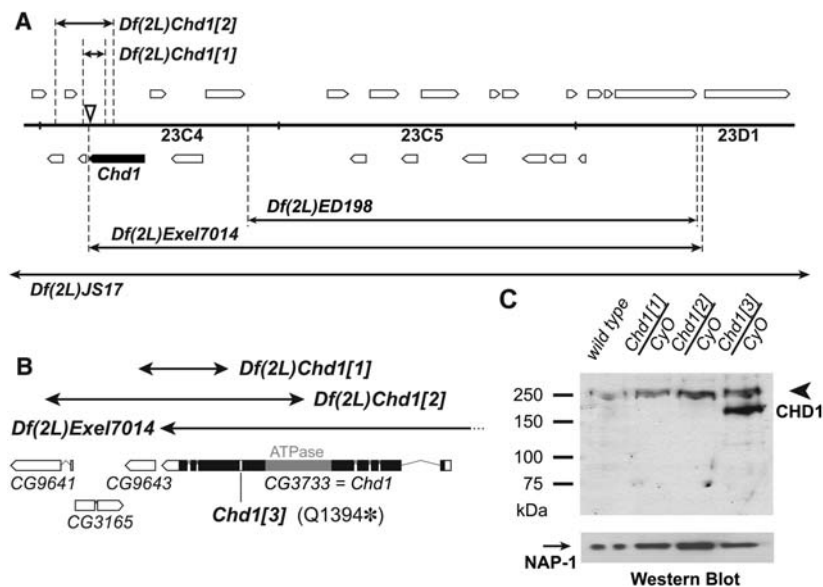


Fig. 1. Characterization of *Chd1* mutant alleles. **(A)** Genomic structure of the *Chd1* locus. *Df(2L)JS17* and *Df(2L)Exel7014* uncover *Chd1*. White boxes, predicted genes; black box, *Chd1*; black arrows, chromosome deficiencies; dashed lines, deficiency breakpoints; triangle, *P{EPgy2}EY07345* insertion that was used for excisions. **(B)** The *Chd1[1]* and *Chd1[2]* excisions delete 296 and 958 amino acids, respectively, from the C terminus of CHD1. *Chd1[3]* has a nonsense mutation resulting in a stop at glutamine 1394. The distal breakpoint of *Df(2L)Exel7014* is located immediately downstream of the *Chd1* 3' untranslated region. White boxes, predicted genes; black box, *Chd1* coding sequence; gray box, *Chd1* ATPase domain. **(C)** Western blot of heterozygous mutant embryos. Truncated CHD1 polypeptides are not detected in heterozygous *Chd1[1]* or *Chd1[2]* embryos. Heterozygous *Chd1[3]* embryos express a truncated (residues 1 to 1394) CHD1 polypeptide. Arrowhead, wild-type CHD1 (250 kD); arrow, left, NAP-1 (loading control); *CyO*, second-chromosome balancer.

¹Department of Cell Biology, Albert Einstein College of Medicine, 1300 Morris Park Avenue, Bronx, NY 10461, USA.

²Division of Molecular Biology, BioCenter, Innsbruck Medical University, Fritz-Pregl Strasse 3, A-6020 Innsbruck, Austria.

³Department of Molecular Biology and Biochemistry, Rutgers University, 604 Allison Road, Piscataway, NJ 08854, USA.

⁴Section of Molecular Biology, University of California at San Diego, La Jolla, CA 92093, USA.

*Present address: Stem Cell and Developmental Biology Group, Genome Institute of Singapore, 60 Biopolis Street, S138672, Singapore.

†To whom correspondence should be addressed. E-mail: dfyodoro@aecom.yu.edu, alexandra.lusser@i-med.ac.at

haploid (Fig. 2A). To confirm this observation, we mated wild-type or *Chd1*-null females with males that carried a green fluorescent protein (GFP) transgene. Embryonic DNA was amplified with primers detecting male-specific GFP and a reference gene, *Asf1*. In wild-type embryos, both primer pairs produced polymerase

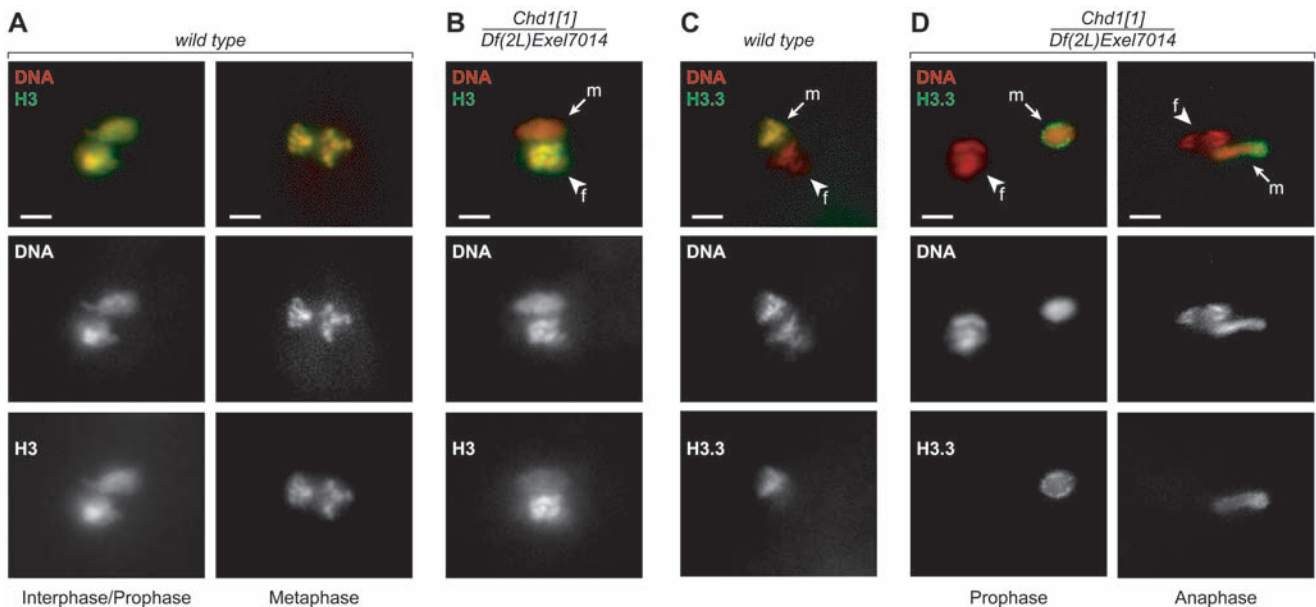
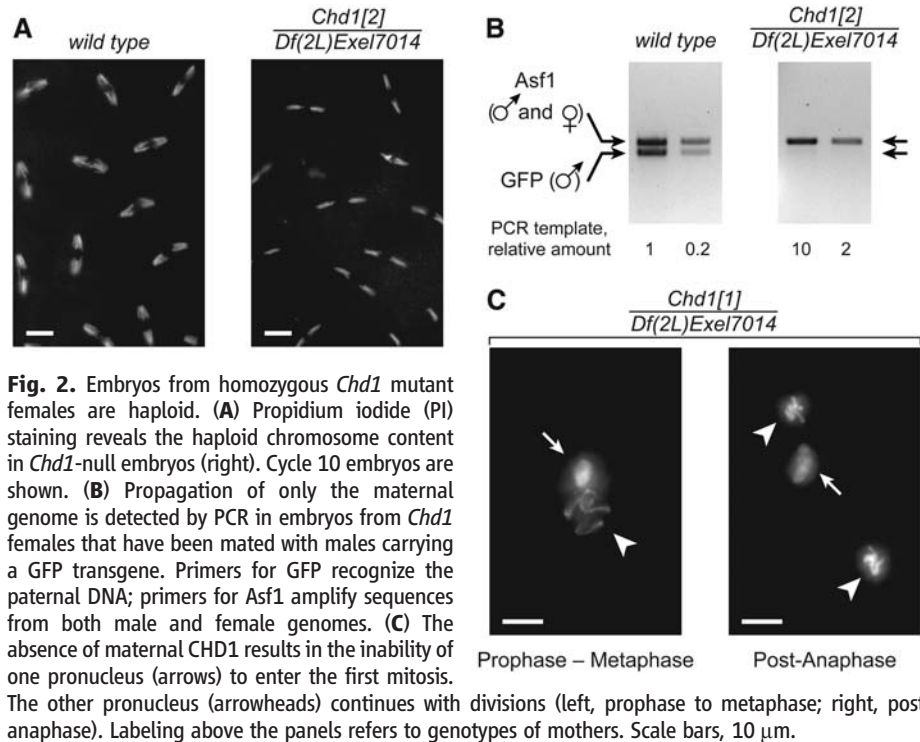
chain reaction (PCR)-amplified products, whereas only the *Asf1* fragment was amplified in the mutants (Fig. 2B). Thus, *Chd1* embryos develop with haploid, maternally derived chromosome content.

To investigate the causes of haploidy in mutant animals, we compared distributions of

various developmental stages in samples of wild-type and *Chd1*-null embryos (table S1). The lack of maternal CHD1 dramatically changed this distribution. Most notably, at 0 to 4 hours after egg deposition, the majority of *Chd1* embryos (56%) remained at a very early stage of development in contrast to the wild type (24%) (table S1).

In *Drosophila* eggs, meiosis gives rise to four haploid nuclei. When the egg is fertilized, one of them is selected as a female pronucleus; the remaining three form the polar body. After breakdown of the sperm nuclear envelope, the compacted sperm chromatin is decondensed, and sperm-specific protamines are replaced with maternal histones. The male and female pronuclei juxtapose in the middle of the embryo and undergo one round of separate haploid mitoses. The resulting products fuse with their counterparts to give two diploid nuclei (12). In the majority of *Chd1* embryos, we observed partial decondensation of the sperm chromatin and normal apposition of parental pronuclei. Then, however, one pronucleus underwent mitosis; the other one did not (Fig. 2C). Considering the subsequent loss of paternal DNA (Fig. 2B), we conclude that mitotic progression of the male pronucleus is hindered in *Chd1* embryos.

Because CHD1 can assemble nucleosomes in vitro, we asked whether the absence of CHD1 affects histone incorporation into the male pronucleus. Embryos from wild-type or *Chd1*-null females were stained with an antibody against histone H3. In wild-type embryos, we observed uniform staining in both parental pronuclei (Fig. 3A). In contrast, in *Chd1*-null embryos only the



the first metaphase. (D) In *Chd1* mutant eggs, H3.3-FLAG accumulates in the periphery of the male pronucleus. The female pronucleus proceeds with mitosis (left, prophase; right, anaphase). (B, C, and D) Arrows, male pronuclei (m); arrowheads, female pronuclei (f). Labeling above the panels refers to genotype of mothers. Red, PI; green, H3 (A and B) or H3.3-FLAG (C and D). Scale bars, 10 μ m.

the first metaphase. (D) In *Chd1* mutant eggs, H3.3-FLAG accumulates in the periphery of the male pronucleus. The female pronucleus proceeds with mitosis (left, prophase; right, anaphase). (B, C, and D) Arrows, male pronuclei (m); arrowheads, female pronuclei (f). Labeling above the panels refers to genotype of mothers. Red, PI; green, H3 (A and B) or H3.3-FLAG (C and D). Scale bars, 10 μ m.

female chromatin was brightly stained. The male pronucleus contained considerably less histone H3 (Fig. 3B). These observations indicate that CHD1 is necessary for nucleosome assembly during sperm decondensation.

Sperm DNA does not replicate during decondensation, and histones are deposited by replication-independent assembly mechanisms, which involve the variant histone H3.3 but not canonical H3 (13). It has been shown in *Drosophila* and mice that H3.3 is specifically present in the male pronucleus (14, 15). We analyzed the distribution of H3.3 in embryos derived from *Chd1*-null females that carry a FLAG-tagged H3.3 transgene. In wild-type embryos, we observed colocalization of the H3.3-FLAG signal with male pronuclear DNA during migration and apposition. No H3.3-FLAG was detectable in the maternal pronucleus (Fig. 3C). In *Chd1*-null embryos, the male pronucleus showed altered H3.3-FLAG staining. The signal did not co-localize with the DNA but remained constrained to the nuclear periphery in a sac-shaped pattern (Fig. 3D).

These findings suggest that in the earliest phases of *Drosophila* development CHD1 is essential for the incorporation of H3.3 and normal assembly of paternal chromatin. In contrast, CHD1 does not appear to affect the organization of maternal chromatin. We conclude that CHD1 is required for replication-independent nucleosome assembly in the decondensing male pronucleus, but is dispensable for replication-coupled incorporation of H3.

It was shown recently that the *sèsame* (*ssm*) mutation of *Drosophila* histone chaperone HIRA caused the development of haploid embryos and abolished H3.3 deposition into the male pro-

nucleus (14). *Chd1* and *ssm* mutants, however, differ profoundly in the manifestation of this phenotype. In *ssm* embryos, H3.3 is absent from the male pronucleus. In contrast, in *Chd1*-null embryos, H3.3 delivery to the male pronucleus appears to be unaffected. Thus, our observations allow us to mechanistically discern the roles of CHD1 and HIRA. Whereas HIRA is essential for histone delivery to the sites of nucleosome assembly, CHD1 directly facilitates histone deposition (fig. S3). Our findings are consistent with observations in vitro that histone chaperones either do not assemble nucleosomes or assemble them at a greatly reduced rate in the absence of ATP-utilizing factors. Our data provide evidence that histone deposition in vivo also transpires through an ATP-dependent mechanism.

CHD1 has been implicated in transcription elongation-related chromatin remodeling (16). We demonstrate that CHD1 functions in nucleosome assembly in the early *Drosophila* embryo, which is transcriptionally silent. The biological role of CHD1, therefore, is not confined to transcription-related processes. The *Schizosaccharomyces pombe* homolog of CHD1, Hrp1, has been shown to function in loading of the centromere-specific H3 variant CENP-A (17). Similarly to H3.3, incorporation of CENP-A into chromatin is not restricted to S phase. Therefore, CHD1 may have a general role in replication-independent nucleosome assembly.

Sperm decondensation involves not only histone incorporation, but also eviction of protamines. To discern whether CHD1 has a role in this process, we analyzed the fate of protamine B (Mst35Bb) in *Chd1*-null embryos. Although we detected GFP-tagged Mst35Bb in the sperm head immediately upon fertilization, we did not observe

Mst35Bb-GFP signal in the male pronucleus (fig. S2). Thus, like HIRA (18), CHD1 is dispensable for protamine removal. We have shown that the male pronucleus in *Chd1*-null embryos contains very low amounts of histones (Fig. 3), yet the DNA is not packaged with protamines. It remains an open question whether other DNA-protein complexes exist in the male pronucleus.

Drosophila eggs contain stores of both known chromatin assembly factors CHD1 and ISWI (fig. S4A) (19). Nevertheless, ISWI is unable to substitute for CHD1 in the deposition of H3.3. To examine whether CHD1 and ISWI differ in their ability to interact with the H3.3 chaperone HIRA, we performed coimmunoprecipitation experiments with extracts from embryos expressing FLAG-HIRA. CHD1 signal was readily detected in FLAG-specific immunoprecipitates, whereas ISWI did not coimmunoprecipitate with HIRA (fig. S4B). Thus, a fraction of CHD1, but not ISWI, physically associates with HIRA. This property of CHD1 may account for its unique function in the H3.3 deposition process.

A subpopulation of *Chd1* mutant haploid embryos survives beyond apposition stage (table S1). Therefore, we asked whether H3.3 deposition is altered in *Chd1* mutant embryos during later developmental stages. In wild-type nuclei, the H3.3-FLAG signal originating from the male pronucleus becomes undetectable after 2 to 3 divisions. Most maternal H3.3 remains distributed diffusely throughout the syncytium. After cycle 11 (roughly correlating with the onset of zygotic transcription) H3.3-FLAG is redistributed into the nuclei, where it colocalizes with the DNA (Fig. 4A). In contrast, incorporation of H3.3 into *Chd1* mutant nuclei was impaired. H3.3-FLAG produced a speckled staining with numerous bright dots that poorly overlapped with the maxima of DNA staining (Fig. 4B). It is important to note that, in the *ssm* (HIRA) mutant, H3.3 incorporation defects in tissues or developmental stages other than the apposition stage were not observed. This result is consistent with the idea that misincorporation of H3.3 in *Chd1* embryos is a direct effect of CHD1 deletion rather than a consequence of haploid development. We also conclude that CHD1 functions in H3.3 deposition during later stages of embryonic development, possibly in a HIRA-independent fashion.

This study provides evidence that ATP-dependent mechanisms are used for histone deposition during chromatin assembly in vivo. Thus, molecular motor proteins, such as CHD1, function not only in remodeling of existing nucleosomes but also in de novo nucleosome assembly from DNA and histones. Finally, our work identifies CHD1 as a specific factor in the assembly of nucleosomes that contain variant histone H3.3.

References and Notes

1. J. Jin et al., *Trends Biochem. Sci.* **30**, 680 (2005).
2. S. Henikoff, K. Ahmad, *Annu. Rev. Cell Dev. Biol.* **21**, 133 (2005).

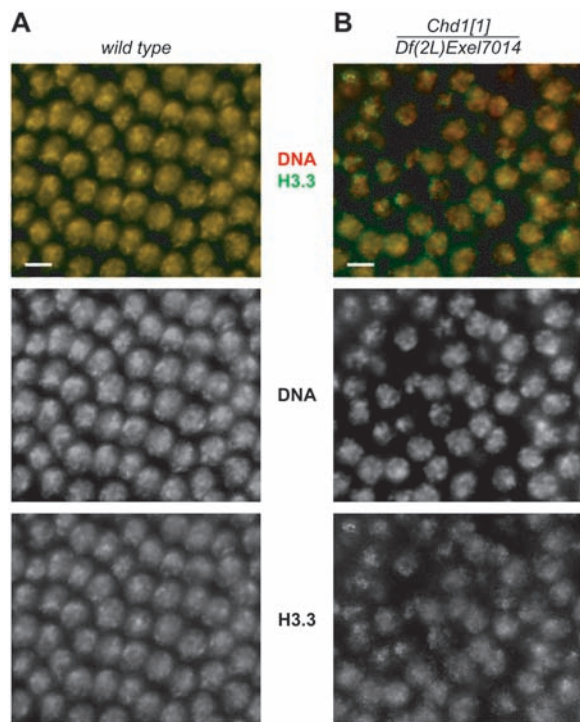


Fig. 4. Deposition of H3.3 into chromatin during syncytial blastoderm is compromised in *Chd1* mutants. **(A)** H3.3-FLAG overlaps with DNA in syncytial nuclei of a cycle 14 wild-type embryo. **(B)** H3.3-FLAG colocalizes poorly with DNA in *Chd1* mutant embryos. Labeling above the panels refers to genotypes of mothers. Red, PI; green, H3.3-FLAG. Scale bars, 10 μ m.

3. D. V. Fyodorov, J. T. Kadonaga, *Cell* **106**, 523 (2001).
4. H. Tagami, D. Ray-Gallet, G. Almouzni, Y. Nakatani, *Cell* **116**, 51 (2004).
5. T. Ito *et al.*, *Genes Dev.* **13**, 1529 (1999).
6. P. D. Varga-Weisz *et al.*, *Nature* **388**, 598 (1997).
7. A. Loyola *et al.*, *Mol. Cell. Biol.* **23**, 6759 (2003).
8. T. Woodage, M. A. Basrai, A. D. Baxevasis, P. Hieter, F. S. Collins, *Proc. Natl. Acad. Sci. U.S.A.* **94**, 11472 (1997).
9. A. Lusser, D. L. Urwin, J. T. Kadonaga, *Nat. Struct. Mol. Biol.* **12**, 160 (2005).
10. Materials and methods are available as supporting material on Science Online.
11. For *Drosophila* genetics information, see FlyBase.org.
12. G. Callaini, M. G. Riparbelli, *Dev. Biol.* **176**, 199 (1996).
13. K. Ahmad, S. Henikoff, *Mol. Cell* **9**, 1191 (2002).
14. B. Loppin *et al.*, *Nature* **437**, 1386 (2005).
15. M. E. Torres-Padilla, A. J. Bannister, P. J. Hurd, T. Kouzarides, M. Zernicka-Goetz, *Int. J. Dev. Biol.* **50**, 455 (2006).
16. R. J. Sims 3rd, R. Belotserkovskaya, D. Reinberg, *Genes Dev.* **18**, 2437 (2004).
17. J. Walfridsson *et al.*, *Nucleic Acids Res.* **33**, 2868 (2005).
18. S. Jayaramaiah Raja, R. Renkawitz-Pohl, *Mol. Cell. Biol.* **25**, 6165 (2005).
19. R. Deuring *et al.*, *Mol. Cell* **5**, 355 (2000).
20. We thank M. Goralik-Schramel for technical assistance; B. Loppin and R. Renkawitz-Pohl for fly lines; and R. Perry for antibodies. We thank K. Beirnt, B. Birshenti, V. Elagin, T. Juven-Gershon, M.-C. Keogh, P. Loidl, S. Moretini, M. Scharff, D. Sharp, and A. Skoultchi for critical reading of the manuscript and A. Tokareva for

discussions and advice. This work was supported by grants from the National Institutes of Health to D.V.F. (GM74233) and J.T.K. (GM58272), the Austrian Science Foundation (Y275-B12) and Tyrolean Science Foundation to A.L., and the Swiss National Science Foundation to V.P. D.V.F. is a Scholar of the Sidney Kimmel Foundation for Cancer Research.

Supporting Online Material

www.sciencemag.org/cgi/content/full/317/5841/1087/DC1
Materials and Methods
Figs. S1 to S5

Table S1
References

17 May 2007; accepted 13 July 2007
10.1126/science.1145339

Blue-Light–Activated Histidine Kinases: Two-Component Sensors in Bacteria

Trevor E. Swartz,^{1*} Tong-Seung Tseng,² Marcus A. Frederickson,¹ Gastón Paris,³ Diego J. Comerci,⁶ Gireesh Rajashekar,^{4,7} Jung-Gun Kim,⁵ Mary Beth Mudgett,⁵ Gary A. Splitter,⁴ Rodolfo A. Ugalde,⁶ Fernando A. Goldbaum,³ Winslow R. Briggs,² Roberto A. Bogomolni^{1†}

Histidine kinases, used for environmental sensing by bacterial two-component systems, are involved in regulation of bacterial gene expression, chemotaxis, phototaxis, and virulence. Flavin-containing domains function as light-sensory modules in plant and algal phototropins and in fungal blue-light receptors. We have discovered that the prokaryotes *Brucella melitensis*, *Brucella abortus*, *Erythrobacter litoralis*, and *Pseudomonas syringae* contain light-activated histidine kinases that bind a flavin chromophore and undergo photochemistry indicative of cysteinyl-flavin adduct formation. Infection of macrophages by *B. abortus* was stimulated by light in the wild type but was limited in photochemically inactive and null mutants, indicating that the flavin-containing histidine kinase functions as a photoreceptor regulating *B. abortus* virulence.

LOV (light, oxygen, or voltage) domains are distributed in the three kingdoms of life (Eukarya, Archaea, and Bacteria) (1, 2). In most cases, the LOV domain is the primary sensory module that conveys a signal to protein domains with known or putative functions as diverse as regulation of gene expression, regulation of protein catabolism, and activation of serine/threonine kinases in eukaryotes and histidine kinases in prokaryotes (3, 4). The only

two LOV-domain proteins from bacteria that have been studied are YtvA—a LOV-STAS (LOV–sulfate transporter and anti-sigma factor antagonist) protein from *Bacillus subtilis*—and a LOV protein (containing no other known domains) from *Pseudomonas putida* (5–8).

The best-characterized LOV domains belong to the plant blue-light receptors, the phototropins, and the closely related photoreceptor neochrome (9). The LOV-domain x-ray structure shows the flavin mononucleotide (FMN) chromophore noncovalently bound to the protein through hydrogen bonding and hydrophobic interactions, and the sulfur atom of a reactive cysteine to be within 4.2 Å of the C(4a) carbon of FMN (10). Light absorption by the LOV-domain flavin chromophore results in formation of a cysteinyl-flavin adduct in which the sulfur of the reactive cysteine forms a covalent bond

with the C(4a) carbon of FMN. In the phototropin LOV domains, this stable bond spontaneously breaks in the dark (in many seconds), completing a photocycle (11). This process has been proposed to be base catalyzed (12–14). Cysteinyl adduct formation in the phototropins produces protein conformational changes (15, 16) that activate a serine/threonine kinase domain, resulting in autophosphorylation (9). The activated phototropins mediate several blue-light responses in plants, including phototropism, chloroplast relocation, leaf expansion, and stomatal opening (17).

Sequence analysis predicts that the genomes of the human/animal facultative intracellular pathogen *Brucella melitensis* (18, 19), the plant pathogen *Pseudomonas syringae* (3, 4), and the marine bacterium *Erythrobacter litoralis* code for proteins that contain a LOV domain at their N terminus, with a histidine kinase occupying the C terminus (LOV-HK). Protein sequence and structural modeling [Swiss model (20)] of these bacterial LOV domains predict that all four LOV-HK proteins will bind a flavin and that all contain a cysteine within a few angstroms of the chromophore. Analysis of published genomes indicates 24 different sequenced bacteria contain genes that code for putative LOV-HKs (1, 4).

The full-length proteins (489 amino acids) from *B. melitensis* (BM-LOV-HK) and *B. abortus* (BA-LOV-HK) contain three distinct domains: a LOV domain at the N terminus, followed by a PAS (Per- Arnt- Sim) domain in the intervening sequence, and a histidine kinase at the C terminus (Fig. 1). Although there are some silent mutations in the genes that encode the LOV-HK in the various *Brucella* species, the protein sequence is identical in *B. melitensis*, *B. abortus*, and *B. suis*. The two LOV-HK proteins from *E. litoralis* (346 amino acids and 368 amino acids in length for EL346-LOV-HK and

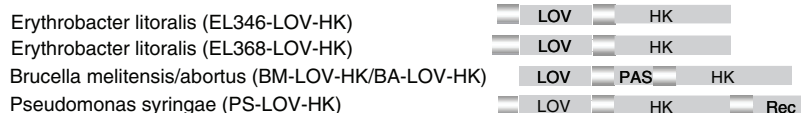


Fig. 1. Domain alignment of LOV histidine kinase proteins (LOV-HK).

¹Department of Chemistry and Biochemistry, University of California, Santa Cruz, Santa Cruz, CA, USA. ²Department of Plant Biology, Carnegie Institution of Washington, Stanford, CA, USA. ³Fundación Instituto Leloir, Instituto de Investigaciones Bioquímicas Buenos Aires–Consejo Nacional de Investigaciones Científicas y Técnicas (IIBBA-CONICET), Buenos Aires, Argentina. ⁴Department of Animal Health and Biomedical Sciences, University of Wisconsin, Madison, WI, USA. ⁵Department of Biological Sciences, Stanford University, Stanford, CA, USA. ⁶Instituto de Investigaciones Biotecnológicas, Universidad Nacional de San Martín, CONICET, San Martín, Argentina. ⁷Food Animal Health Research Program—Ohio Agricultural Research and Development Center (FAHRP-OARDC), Ohio State University, Wooster, OH, USA.

*Present address: Early Stage Pharmaceutical Development, Genentech, Inc., South San Francisco, CA, USA.

†To whom correspondence should be addressed. E-mail: bogo@chemistry.ucsc.edu